

Supplementary Material

Magnetic properties and neutron spectroscopy of lanthanoid- {tetrabromocatecholate/18-crown-6} single-molecule magnets

Maja A. Dunstan^A, Marina Cagnes^B, Wasinee Phonsri^C, Keith S. Murray^C, Richard A. Mole^B and Colette Boskovic^{A,}*

^ASchool of Chemistry, The University of Melbourne, Parkville, Vic. 3010, Australia.

^BAustralian Nuclear Science and Technology Organisation, Locked Bag 2001, Kirrawee, NSW 2232, Australia.

^CSchool of Chemistry, Monash University, Clayton, Vic. 3800, Australia.

*Correspondence to: Email: c.boskovic@unimelb.edu.au

Single crystal X-ray diffraction	S3
Powder X-ray diffraction	S4
Infrared spectroscopy	S6
Thermogravimetric analysis	S8
Light field microscopy	S10
Inelastic neutron scattering spectra of 1-La^D	S12
Phonon Generalized Density of States of 1-La^D	S13
Dynamic magnetic susceptibility of Tb(III) analogues	S14
Dynamic magnetic susceptibility of Dy(III) analogues	S18

Single crystal X-ray diffraction

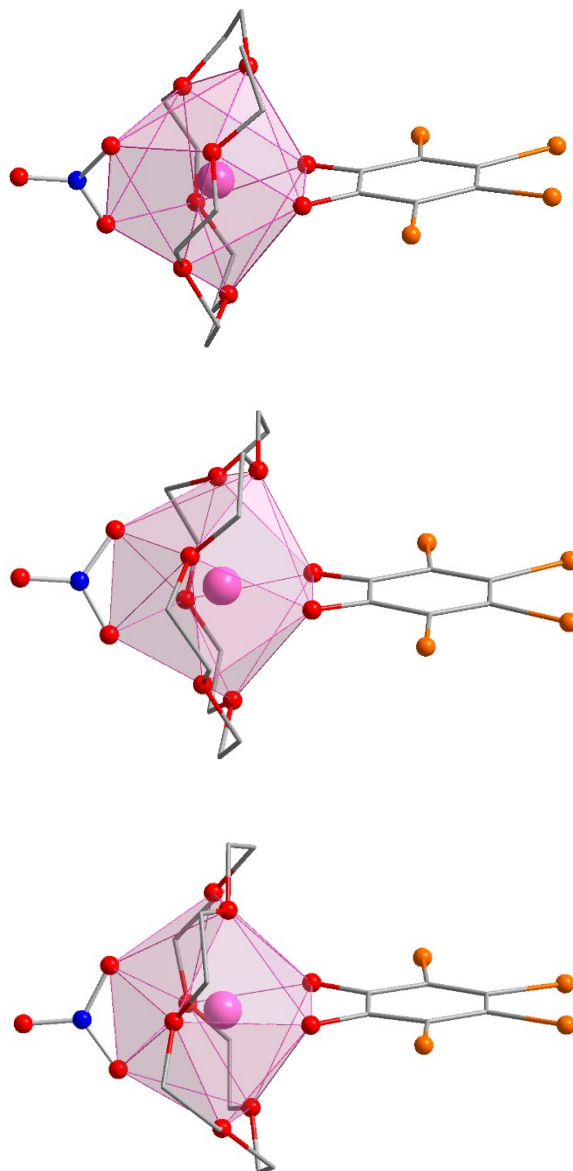


Figure S1: Structural representation of **1-Ln** (upper), **2-Ln** (middle) and **3-Ln** (lower) with the sphenocorona coordination polyhedra highlighted. Hydrogen atoms, disordered parts, and solvent molecules have been omitted for clarity. Colour code: Ln (pink), Br (orange), O (red), N (blue), C (grey).

Powder X-ray diffraction

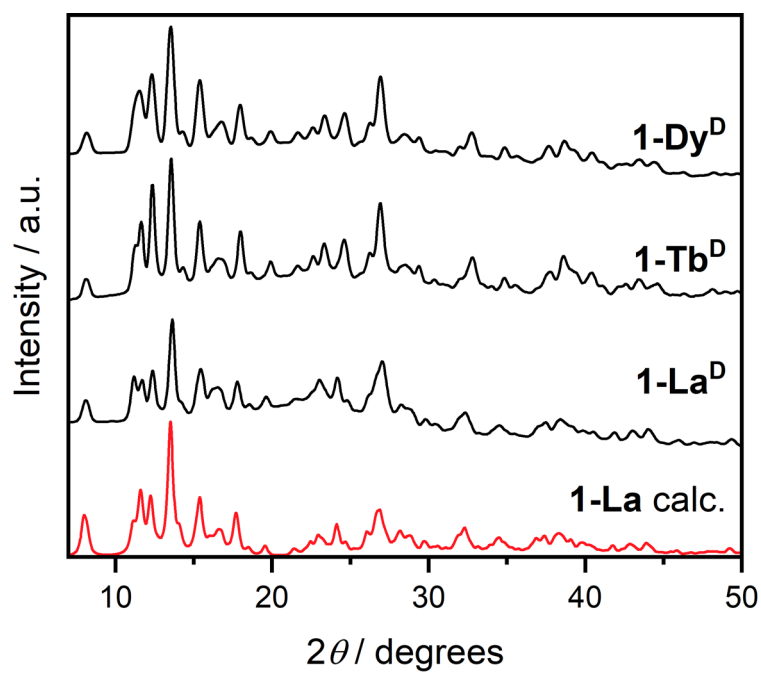


Figure S2: Powder X-ray diffraction data for 1-Ln^D.

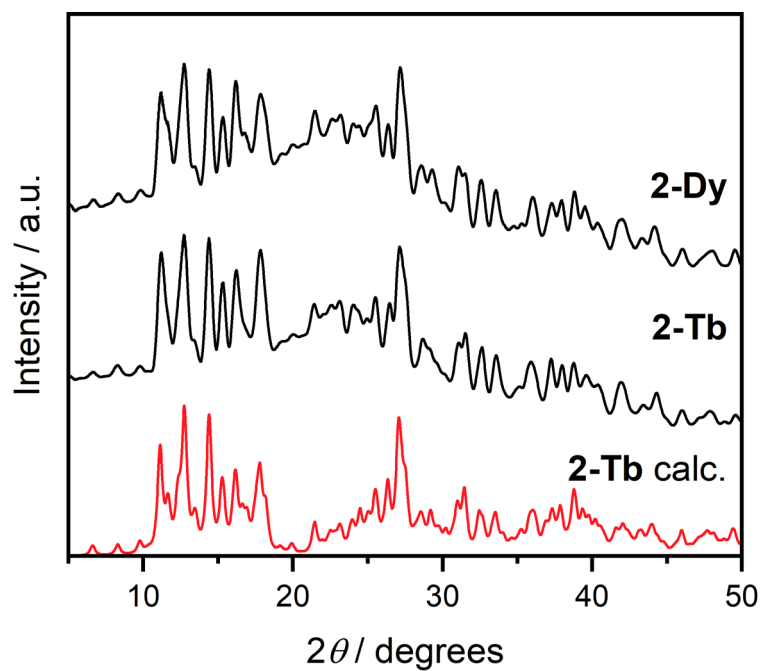


Figure S3: Powder X-ray diffraction data for 2-Ln.

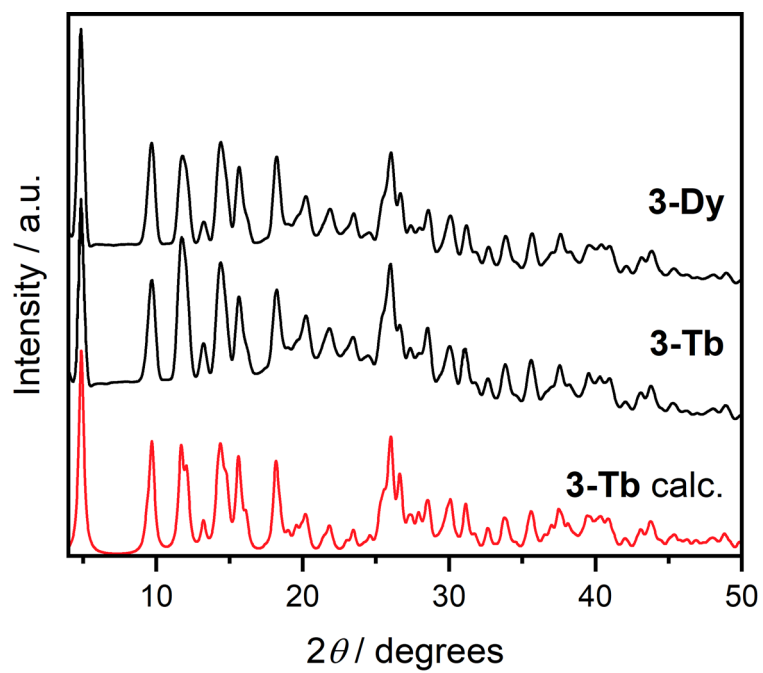


Figure S4: Powder X-ray diffraction data for **3-Ln**.

Infrared spectroscopy

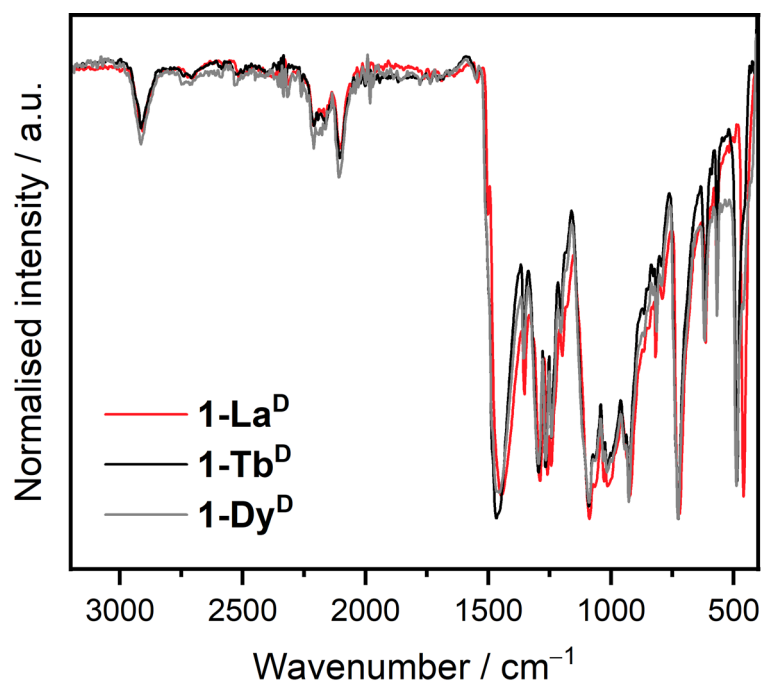


Figure S5: FT-IR (ATR) spectra of **1-Ln^D**.

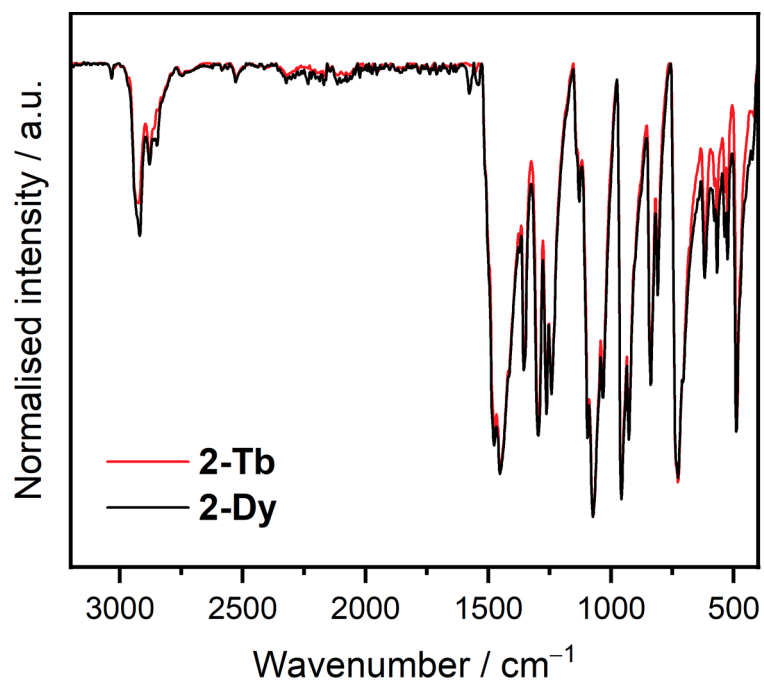


Figure S6: FT-IR (ATR) spectra of **2-Ln**.

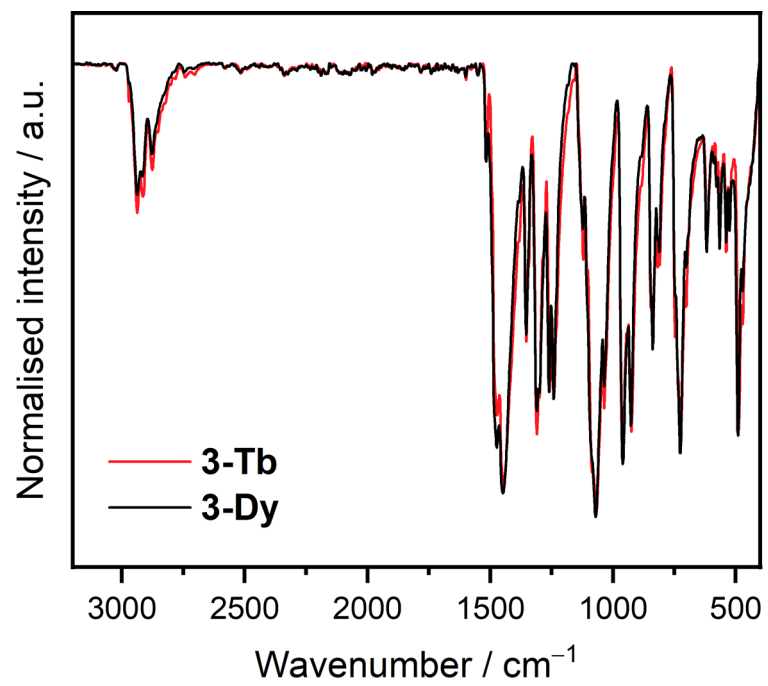


Figure S7: FT-IR (ATR) spectra of **3-Ln**.

Thermogravimetric analysis

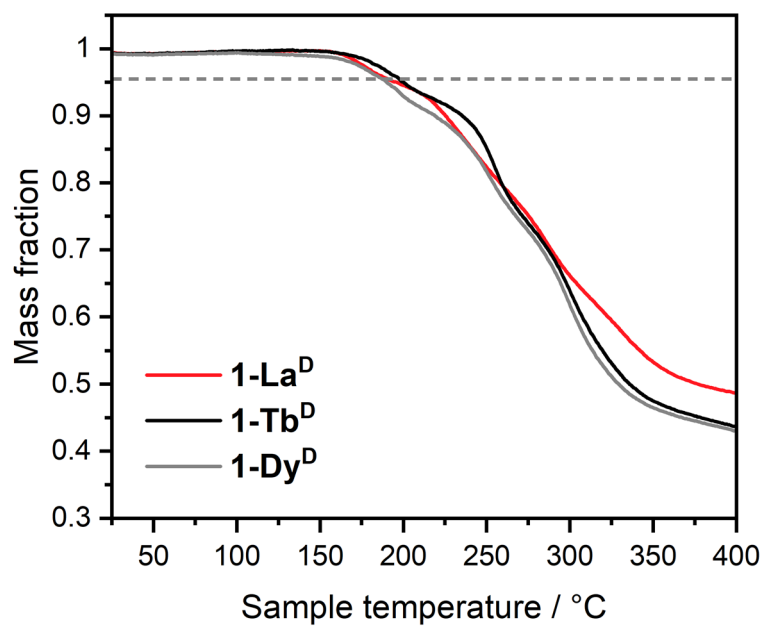


Figure S8: Thermogravimetric analysis of **1-Ln^D**.

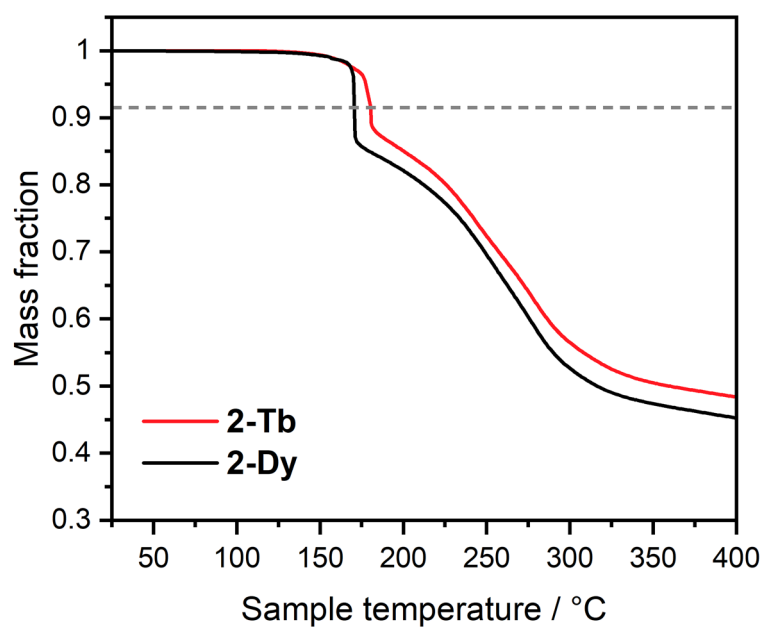


Figure S9: Thermogravimetric analysis of **2-Ln**.

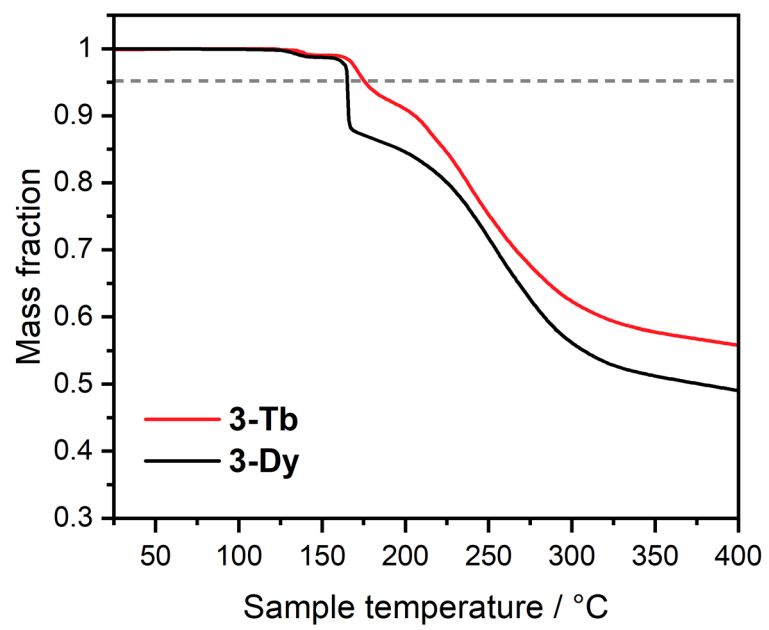


Figure S10: Thermogravimetric analysis of **3-Ln**.

Light field microscopy

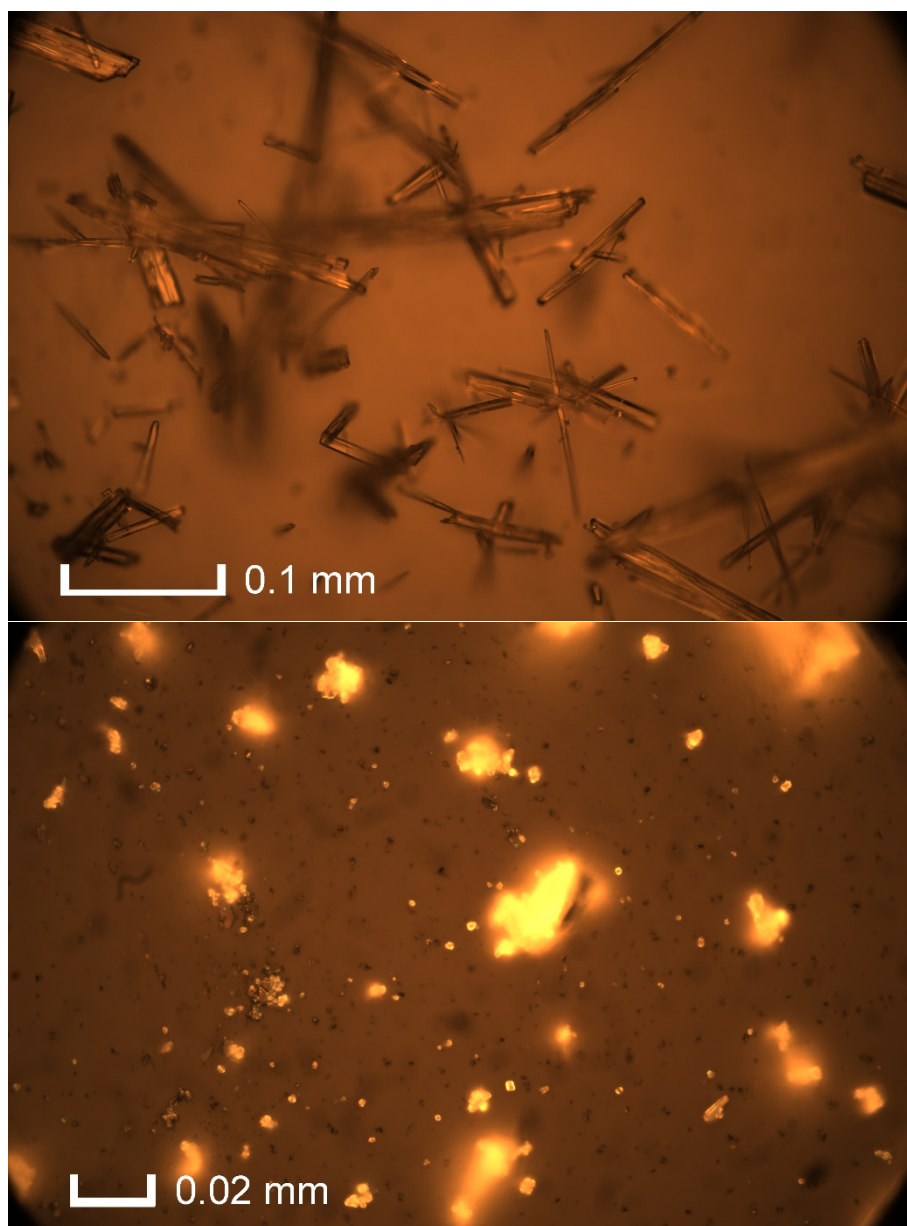


Figure S11: Light field microscope images of **1-Tb^D** (above) and **1-Tb^D-a** (below).

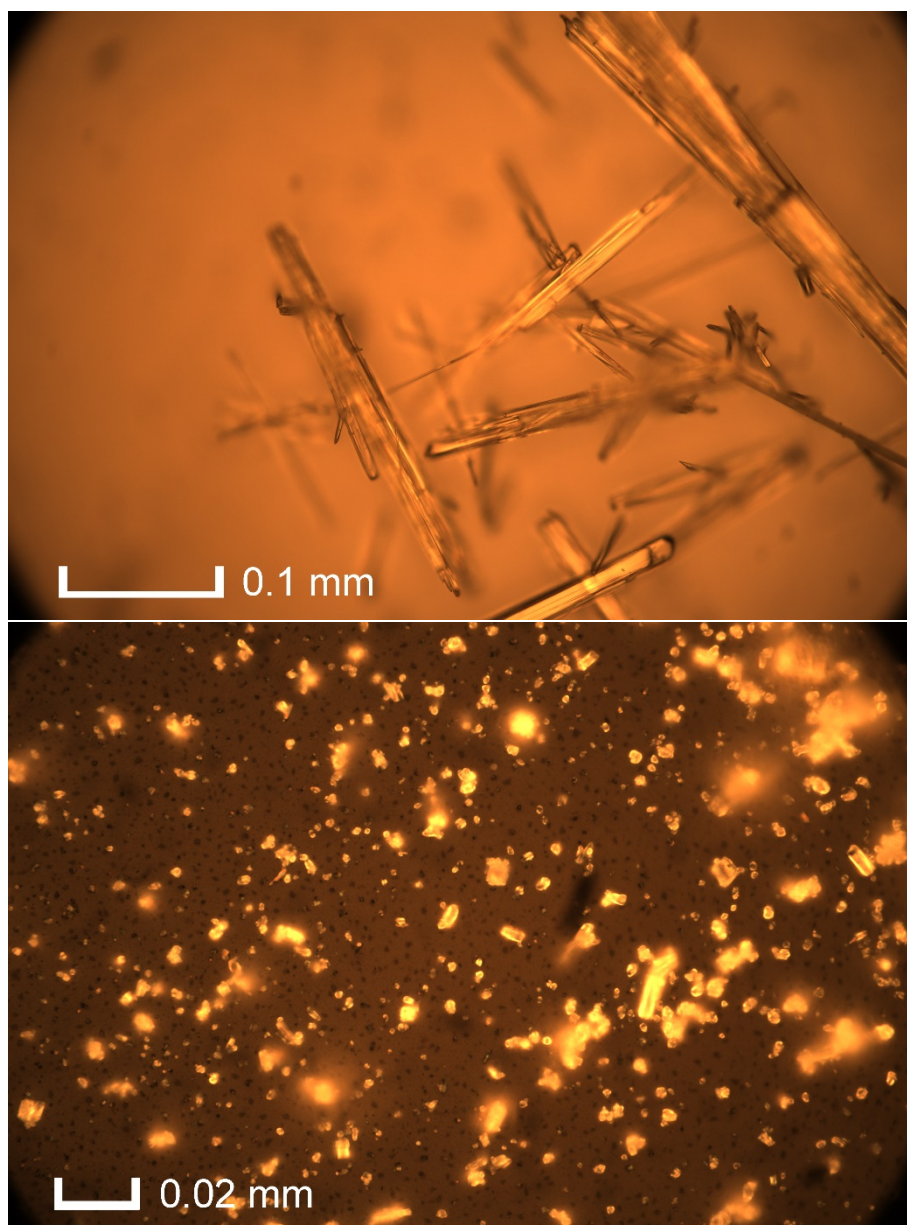


Figure S12: Light field microscope images of **1-Dy^D** (above) and **1-Dy^D-a** (below).

Inelastic neutron scattering spectra of 1-La^D

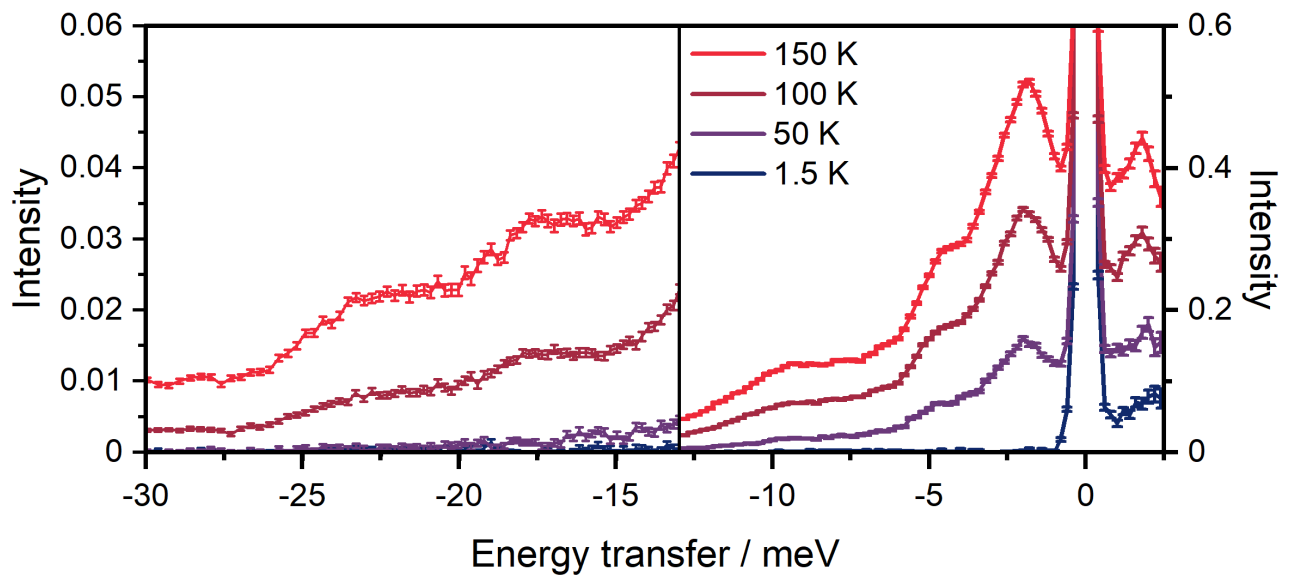


Figure S13: Variable temperature INS spectra of 1-La^D, integrated over all Q .

Phonon Generalized Density of States of 1-La^D

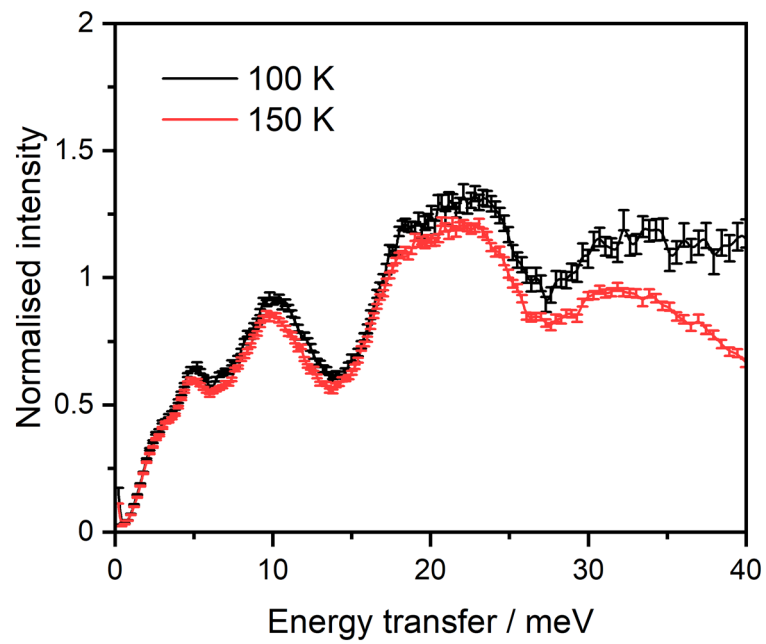


Figure S14: Phonon GDOS calculated for 1-La^D at $T = 100$ K (black) and 150 K (red).

Dynamic magnetic susceptibility of Tb(III) analogues

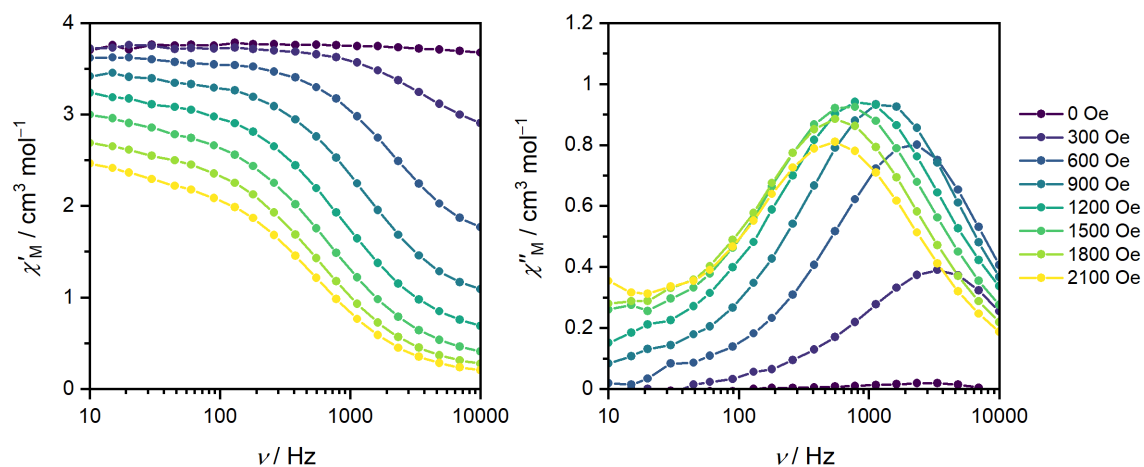


Figure S15: Magnetic field dependence of in-phase and out-of-phase components of the ac molar magnetic susceptibility of **1-Tb^D** measured at $T = 2.5$ K

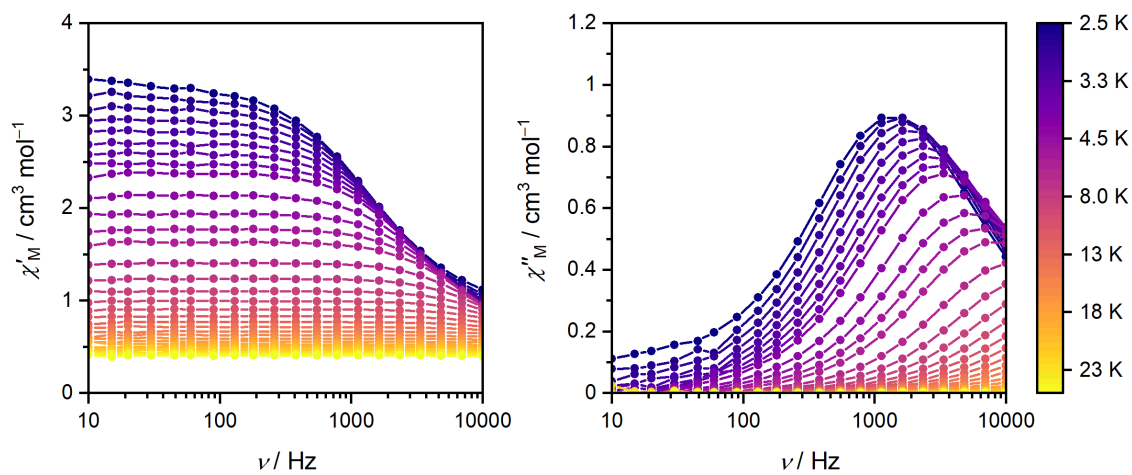


Figure S16: In-phase and out-of-phase components of the ac molar magnetic susceptibility of **1-Tb^D** measured in an applied field of $B_{dc} = 1,000$ Oe.

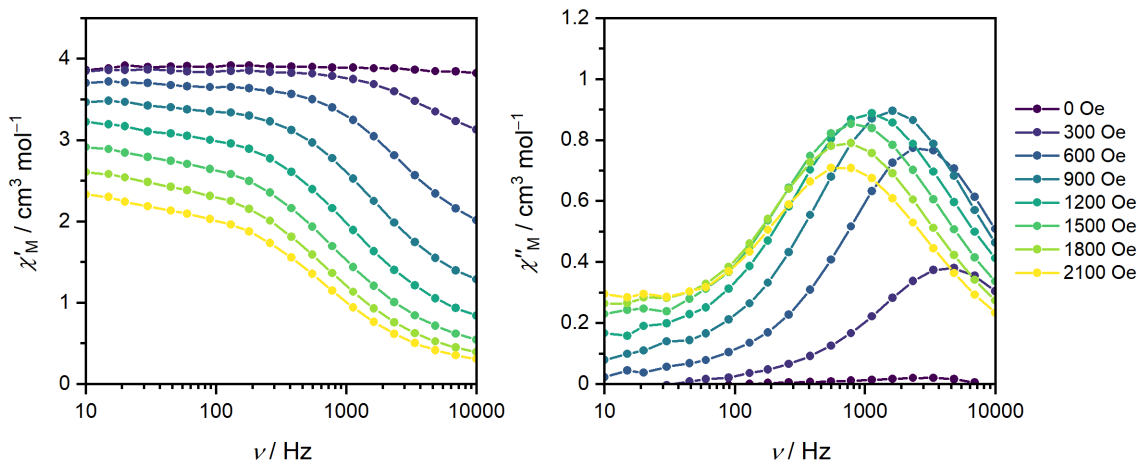


Figure S17: Magnetic field dependence of in-phase and out-of-phase components of the ac molar magnetic susceptibility of **1-Tb^D-a** measured at $T = 2.5$ K

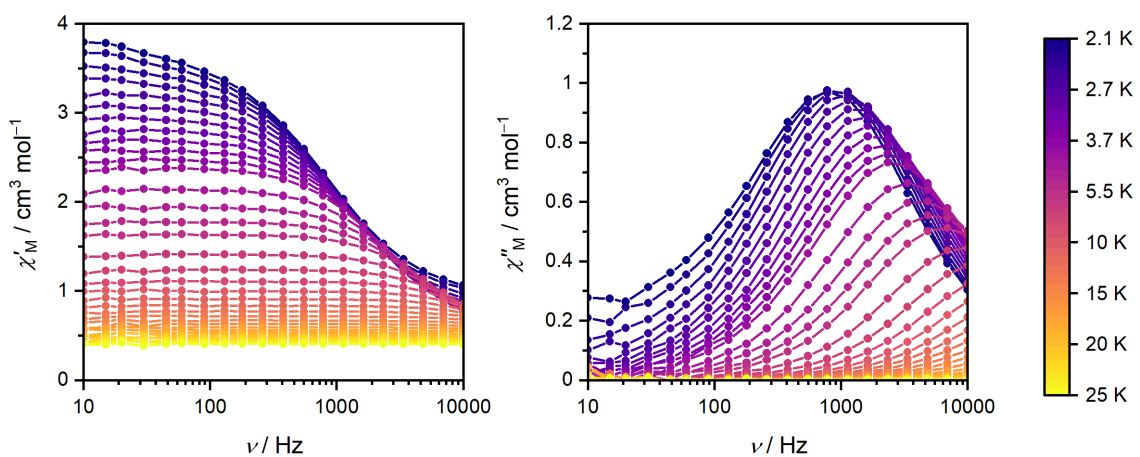


Figure S18: In-phase and out-of-phase components of the ac molar magnetic susceptibility of **1-Tb^D-a** measured in an applied field of $B_{dc} = 1,000$ Oe.

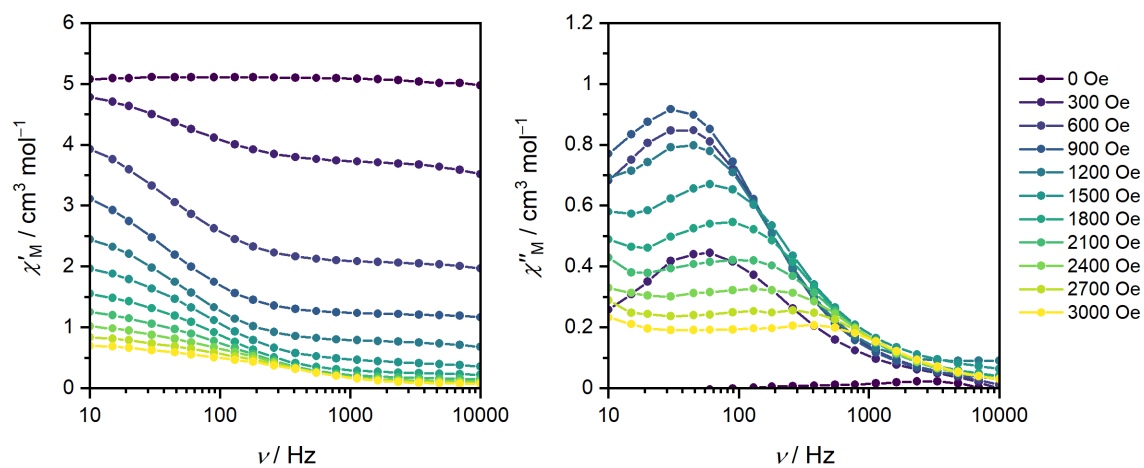


Figure S19: Magnetic field dependence of in-phase and out-of-phase components of the ac molar magnetic susceptibility of **2-Tb** measured at $T = 2.0$ K

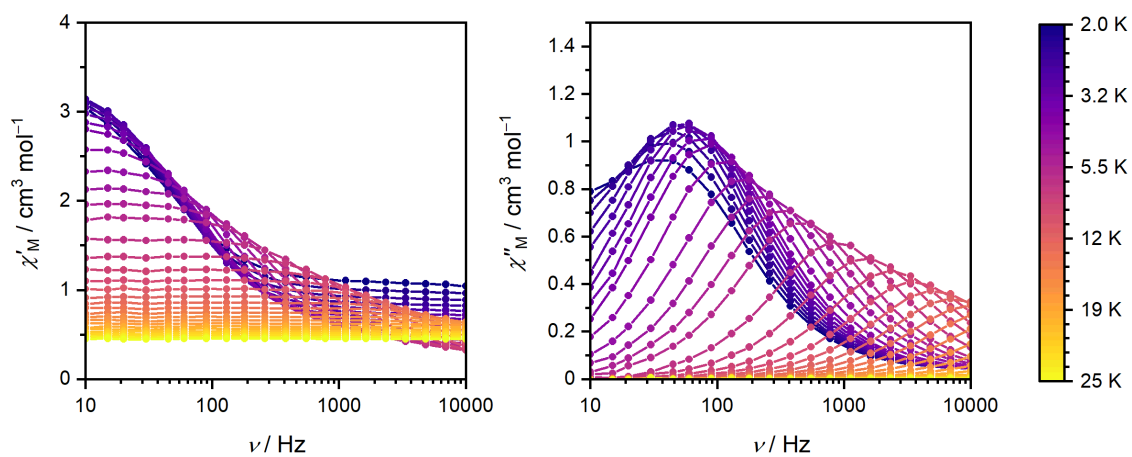


Figure S20: In-phase and out-of-phase components of the ac molar magnetic susceptibility of **2-Tb** measured in an applied field of $B_{dc} = 1,000$ Oe.

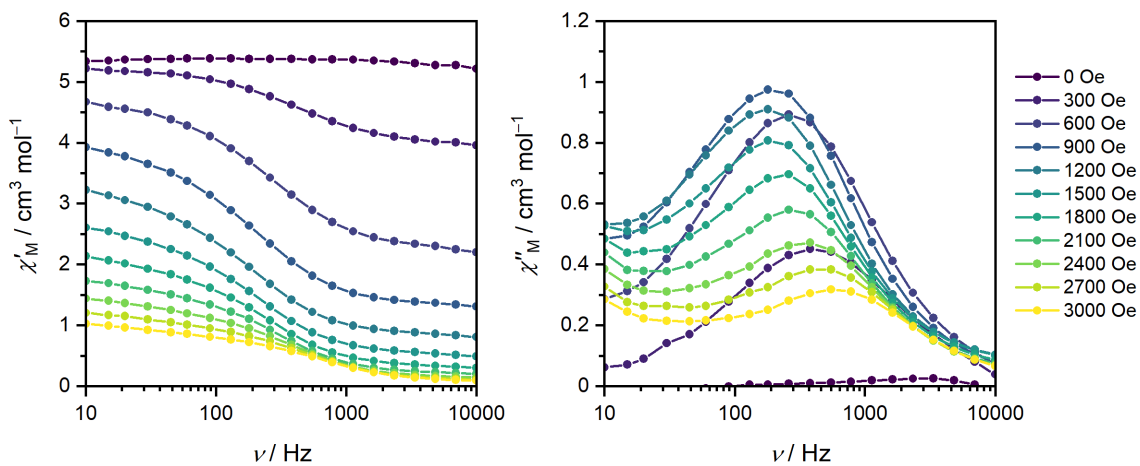


Figure S21: Magnetic field dependence of in-phase and out-of-phase components of the ac molar magnetic susceptibility of **3-Tb** measured at $T = 2.0$ K

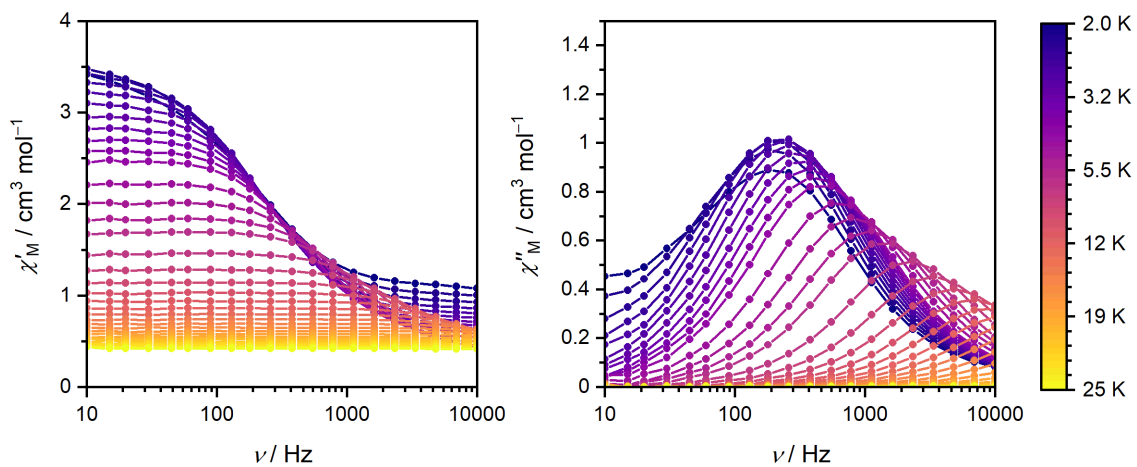


Figure S22: In-phase and out-of-phase components of the ac molar magnetic susceptibility of **3-Tb** measured in an applied field of $B_{dc} = 1,000$ Oe.

Dynamic magnetic susceptibility of Dy(III) analogues

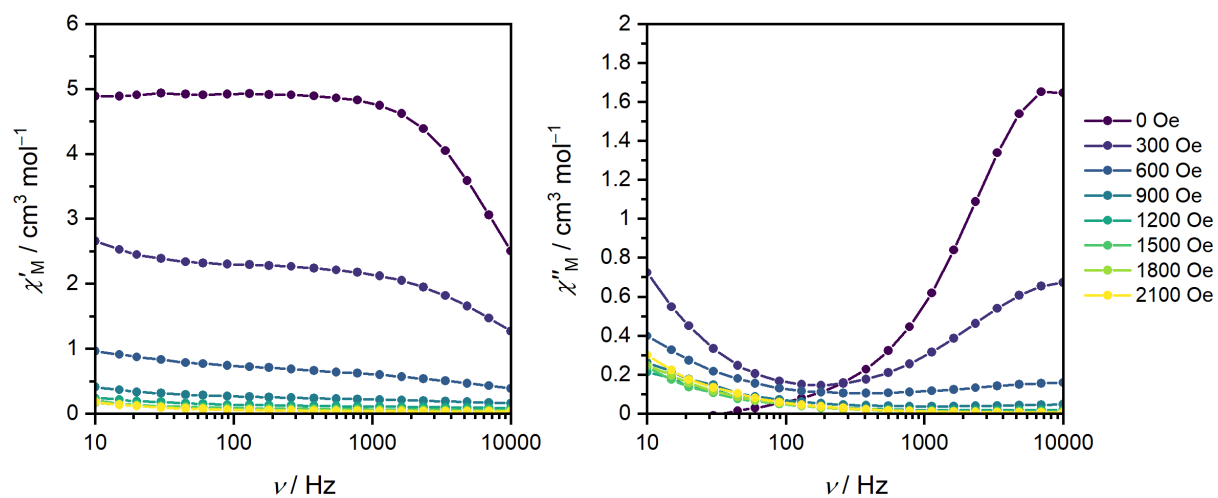


Figure S23: Magnetic field dependence of in-phase and out-of-phase components of the ac molar magnetic susceptibility of **1-Dy^D** measured at $T = 2.5 \text{ K}$

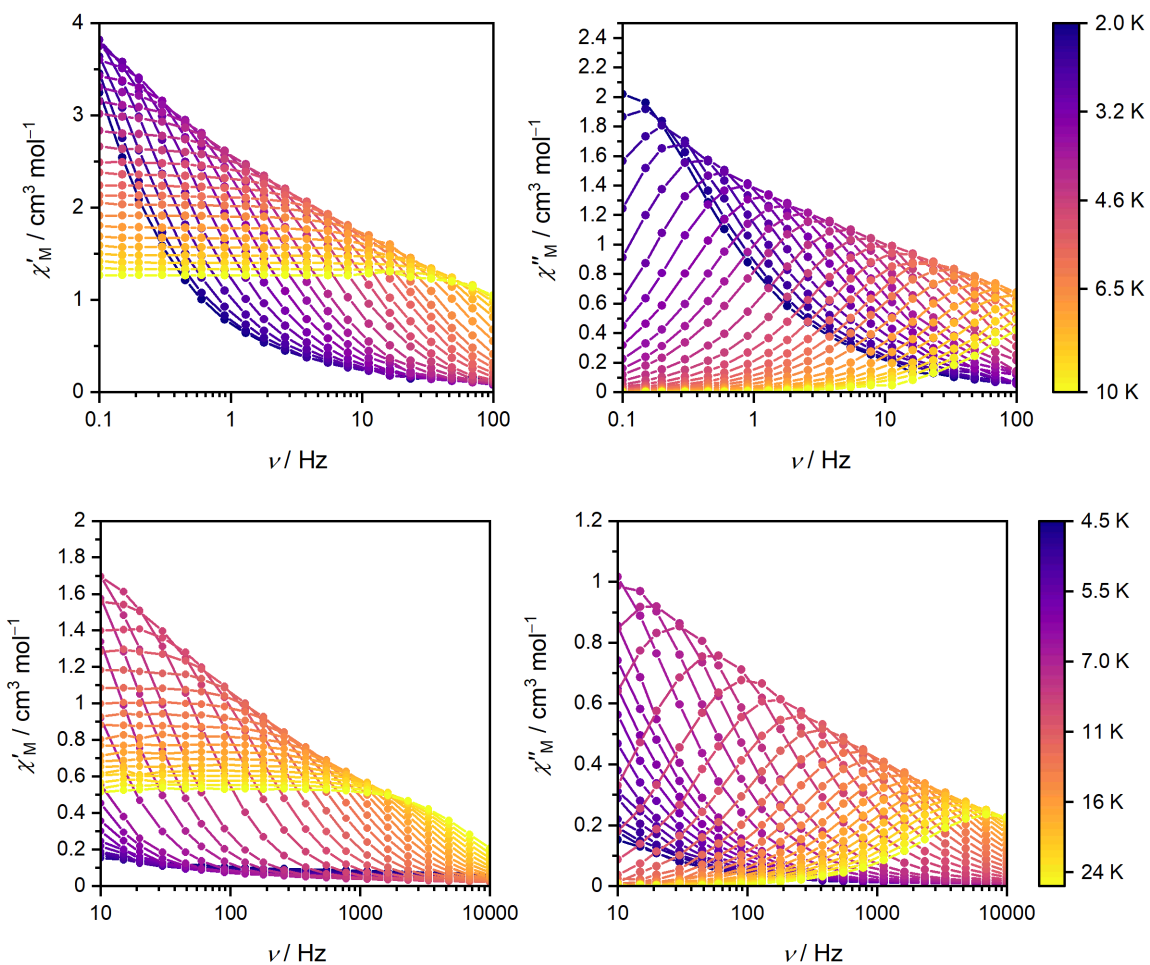


Figure S24: In-phase and out-of-phase components of the ac molar magnetic susceptibility of **1-Dy^D** measured in an applied field of $B_{dc} = 1,500$ Oe.

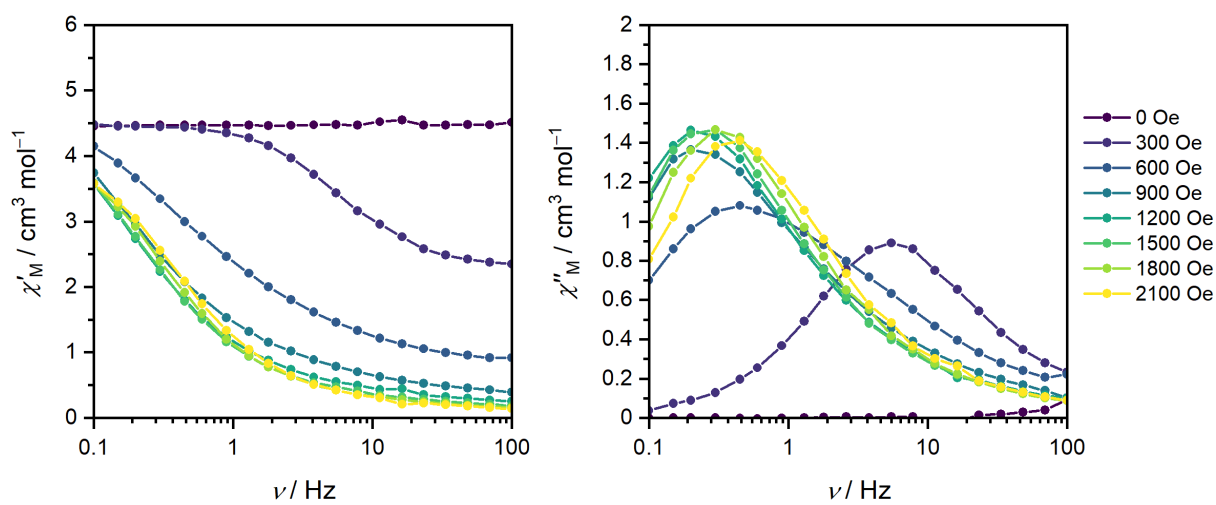


Figure S25 Magnetic field dependence of in-phase and out-of-phase components of the ac molar magnetic susceptibility of **1-Dy^D-a** measured at $T = 2.5$ K

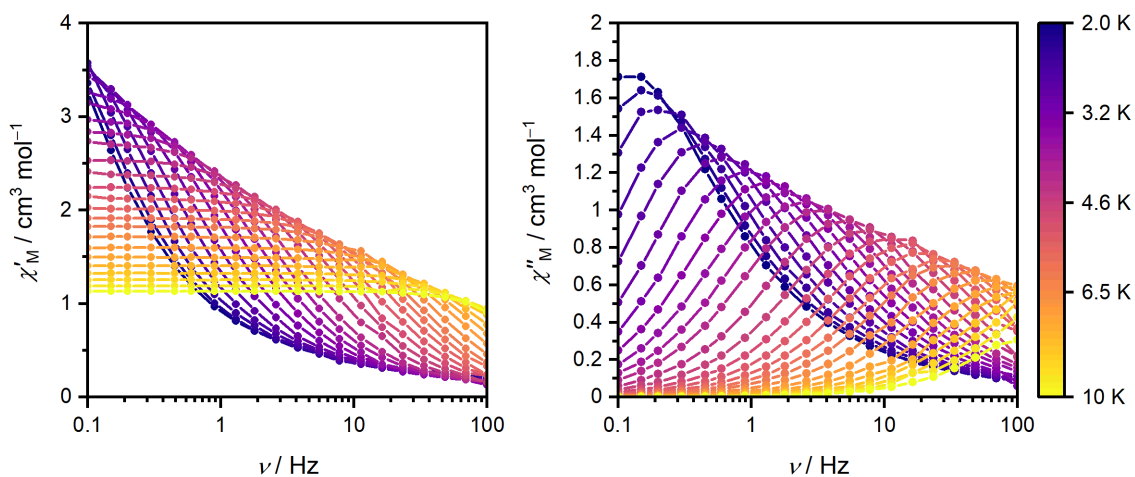


Figure S26: In-phase and out-of-phase components of the ac molar magnetic susceptibility of **1-Dy^D-a** measured in an applied field of $B_{dc} = 1,500$ Oe.

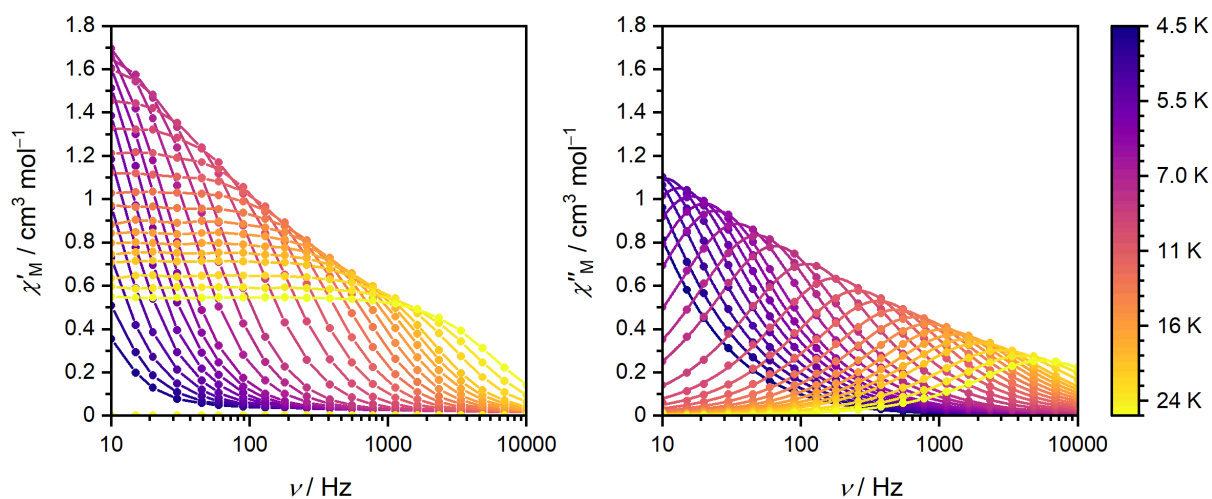


Figure S27: In-phase and out-of-phase components of the ac molar magnetic susceptibility of **2-Dy** measured in an applied field of $B_{dc} = 1,500$ Oe.

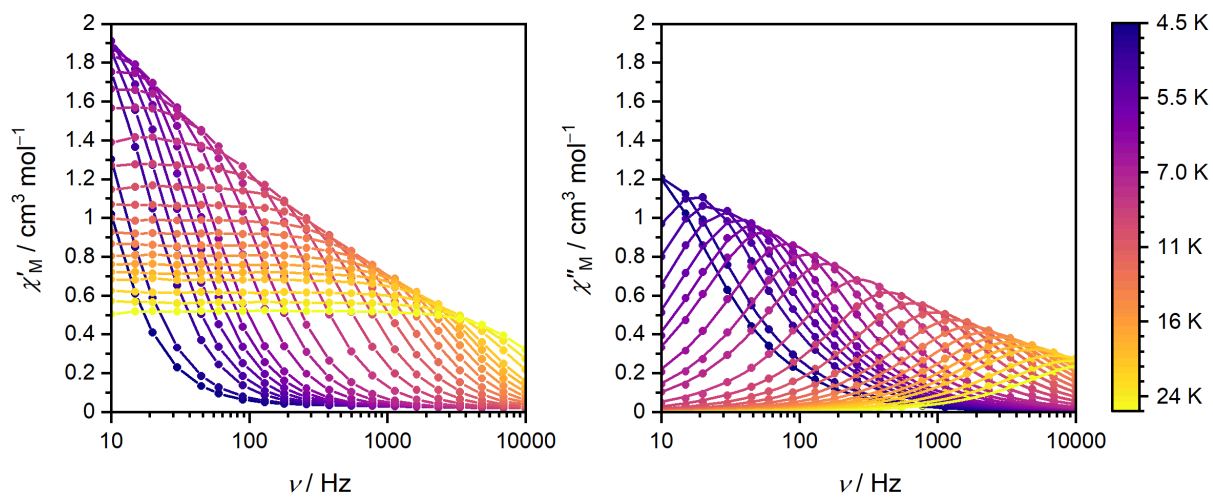


Figure S28: In-phase and out-of-phase components of the ac molar magnetic susceptibility of **3-Dy** measured in an applied field of $B_{\text{dc}} = 1,500$ Oe.